



HAL
open science

Experimental characterization of heat transfer inside a refrigerated trailer loaded with carcasses

Mouna Merai, D. Flick, Laurent Guillier, Steven Duret, Onrawee Laguerre

► To cite this version:

Mouna Merai, D. Flick, Laurent Guillier, Steven Duret, Onrawee Laguerre. Experimental characterization of heat transfer inside a refrigerated trailer loaded with carcasses. *International Journal of Refrigeration*, 2019, 99, pp.194-203. 10.1016/j.ijrefrig.2018.11.041 . hal-02608709

HAL Id: hal-02608709

<https://hal.inrae.fr/hal-02608709>

Submitted on 26 Oct 2021

HAL is a multi-disciplinary open access archive for the deposit and dissemination of scientific research documents, whether they are published or not. The documents may come from teaching and research institutions in France or abroad, or from public or private research centers.

L'archive ouverte pluridisciplinaire **HAL**, est destinée au dépôt et à la diffusion de documents scientifiques de niveau recherche, publiés ou non, émanant des établissements d'enseignement et de recherche français ou étrangers, des laboratoires publics ou privés.



Distributed under a Creative Commons Attribution - NonCommercial 4.0 International License

Experimental characterization of heat transfer inside a refrigerated trailer loaded with carcasses

M. Merai^{1,2,*}, D. Flick², L. Guillier³, S. Duret¹, O. Laguerre¹

¹ Irstea, UR GPAN, Refrigeration Process Engineering Research Unit, 1 rue Pierre-Gilles de Gennes, 92761 Antony, France

² UMR Ingénierie Procédés Aliments, AgroParisTech, INRA, Université Paris-Saclay, 91300 Massy, France

³ Université Paris-Est, Anses, French Agency for Food, Environmental and Occupational Health and Safety, Food Safety Laboratory, 23 avenue du Général de Gaulle, 94706 Maisons-Alfort Cedex, France

* mouna.merai@irstea.fr

Abstract

Measurements of convective heat transfer coefficients on reduced-scale replicates of half pork carcasses were conducted. Measurements were performed on both the muscle and rind sides at three positions: ham, loin and shoulder. The carcasses were placed in the symmetry plane and near the wall of a reduced-scale refrigerated trailer with or without air distribution ducts. The convective heat transfer coefficient values varied significantly along the trailer in both configurations (with or without air duct). Differences were observed between the rind and muscle sides for all positions. The heat transfer coefficients of the ham part were higher than those of the loin and shoulder parts. An analysis was conducted by correlating the measured convective heat transfer coefficients with the air velocity fields measured by Laser Doppler Velocimetry presented in a previous study.

Keywords: convective heat transfer coefficient, pork carcass, refrigeration, transport, trailer

Nomenclature

a	Nusselt's correlation coefficient
A	heat transfer surface area [m ²]
b	Nusselt's correlation exponent
g	gravitational acceleration [m.s ⁻²]
Gr	Grashof number
h	convective heat transfer coefficient (CHTC) [W.m ⁻² .K ⁻¹]
L	characteristic length [m]
Nu	Nusselt number
Pr	Prandtl number
q	heat flow through the surface [W]
Re	Reynolds number
T _{air}	air temperature [K]
T _s	carcass surface temperature [K]
v	air velocity [m.s ⁻¹]
\dot{V}	volume airflow rate [m ³ .h ⁻¹]
x*	dimensionless position along the trailer length (x* = x/L)
ν	kinematic viscosity of air [m.s ⁻²]
λ	thermal conductivity of air [W.m ⁻¹ .K ⁻¹]
μ	dynamic viscosity of air [kg.m ⁻¹ .s ⁻¹]
ρ	air density [kg.m ⁻³]
β	thermal expansion coefficient [K ⁻¹]
ΔT	temperature difference [K]

Indices

1/2	half airflow rate
ave	average value
i	height position on the carcass
j	side position on the carcass
k	lateral position in the carcass
l	longitudinal position in the truck
m	blowing configuration
max	maximum value
min	minimum value
f	full scale
r	reduced scale

1. Introduction

In order to prevent pathogenic bacteria growth in meat during slaughter operations, legislation requires the application of refrigeration immediately after post mortem inspection of carcasses. However, it is important to control the kinetics of product temperature reduction in order to optimize meat maturation (ensuring good technological quality, i.e. tenderness) and sanitary quality (Savell et al., 2005). In addition, failure to understand the phenomena taking place in the equipment results in excessive weight loss, reduced shelf life or deterioration in product quality (James, 1996, Duret et al., 2014).

French and European regulations have been enforced for the temperature of meat carcasses before and during transportation (Anonymous, 2004). According to this regulation, the meat must be chilled to reach a core temperature of 7°C as soon as possible. This refrigeration must be performed in the cold rooms of the slaughterhouse before any carcass handling operation such as transport or cutting. Derogations have been adopted in some countries to allow the transport of carcasses or half-carcasses with a core temperature above 7°C, if the transport duration is less than 2 hours. In 2014, EFSA adopted a scientific opinion concluding that the surface temperature is an appropriate indicator of bacterial growth. This is related to the fact that aerobic bacteria are essentially on the surface of pork carcasses. Certain aerobic bacteria, especially *Pseudomonas* spp., can reach critical levels much faster than pathogenic bacteria; their growth kinetics may be an indicator of temperature abuse during storage and transport.

It is to be emphasized that the transport of a product in a refrigerated trailer is complex because of the high heterogeneity of air temperature and velocity. Lower product temperatures are often observed at the front, while higher temperatures are observed at the rear close to the doors (Moureh and Flick, 2005). The position of potential sanitary risk (high-temperature zone) can be influenced by the trailer design, the carcass arrangement and the loading density. Thus, an understanding of the airflow and the convective heat transfer coefficient (CHTC) variation at different positions is essential in order to allow the identification of risk zones (areas with low air velocities and low CHTC). An experimental study of airflow in a trailer loaded with pork carcasses has been previously conducted using LDV (Laser Doppler Velocimetry) (Merai et al., 2018). The present work completes this study by investigating the thermal exchange between the air circulating in the trailer and the carcasses at different positions.

Measurements of the CHTC for simple geometries (cylinders, spheres...) and different dimensions have been investigated in the past and reported in the literature (Ghisalberti, 1999), and the effects of air velocity, turbulent intensity and the angle of the object with respect to the airflow have also been investigated. To estimate the overall CHTC between the air and the surface of the carcasses, Kondjoyan (2006) likened the carcasses to cylinders. This author also reported the effect of product dimensions and orientation on the CHTC values. The assumption that the real product geometry can be considered as a simple shape and the use of an overall uniform heat transfer coefficient instead of local values implies significant uncertainties regarding refrigeration kinetics prediction (Kondjoyan and Daudin, 1997).

Several studies were conducted in order to measure the CHTCs on one carcass or a part of a carcass (Harris et al., 2004, Willix et al., 2006, Kondjoyan and Daudin, 1997). The most commonly used method is based on measurements under stationary conditions using flux-meters and thermocouples located in different zones of the carcass surface.

Regardless of the studied carcass type, pork (Kondjoyan et Daudin, 1997), beef (Willix et al., 2006) or lamb (Harris et al, 2004), results showed that the air velocity and the turbulent intensity had a significant effect on the measured CHTC. Moreover, the CHTC values were significantly different depending on the measurement zone. The parts of the carcasses that were more exposed to the airflow showed higher values. Differences between the maximum and minimum values reached an average of 140% (Willix et al., 2006).

The purpose of this study was to measure CHTCs on the surface of carcasses loaded in a refrigerated trailer. Unlike previous studies (Harris et al., 2004, Willix et al., 2006, Kondjoyan and Daudin, 1997), this work does not focus on a single carcass with imposed upstream air characteristics, but instead focuses on carcasses located close to each other in the complex airflow pattern of a trailer. Because of limitations linked to feasibility and the cost of conducting experiments in the field with real carcasses in a real trailer, the experiments were performed in a reduced-scale trailer loaded with reduced-scale carcasses. The heat transfer coefficient was measured on different parts of instrumented carcasses (ham, loin and shoulder) throughout the reduced-scale trailer. Two trailer configurations were studied (with or without air ducts) and the heat transfer coefficient values obtained were compared. Also, the results obtained were correlated with the airflow pattern inside both configurations using the data presented in a previous study (Merai et al., 2018).

2. Material and methods

2.1. Experimental device

2.1.1. Trailer filled with carcasses

The studied transport configuration (number of rails and carcasses, layout) was chosen according to the most common configurations encountered in the long-distance transport of pork carcasses (Figure 1a) observed by our partners, the French Pork Institute (IFIP) and the French Meat Association (Culture Viande). In this configuration, the refrigerated trailer had an internal length of 13.3 m and was loaded with 430 half- carcasses hung on 5 rails (Figures 1b and 1c).

To conduct our experiments within reasonable dimensions, a reduced-scale trailer with a reduced-scale/full-scale ratio of 1:3.3 (745 x 757 x 4000 mm) was used. In order to obtain the same airflow pattern at a reduced scale as at full scale, the inlet velocity of the reduced-scale trailer was adjusted in order to maintain the same Reynolds number as under full-scale conditions.

Even though the air was warmer in the reduced-scale trailer ($\approx 20^\circ\text{C}$) than in a full-scale trailer, the physical properties of the air can be considered almost identical ($\rho_f \approx \rho_r$ and $\mu_f \approx \mu_r$), thus:

$$\text{Re}_f = \text{Re}_r \leftrightarrow \frac{\rho_f V_f L_f}{\mu_f} = \frac{\rho_r V_r L_r}{\mu_r} \rightarrow \frac{V_r}{V_f} = \frac{\dot{V}_f}{\dot{V}_r} = \frac{L_f}{L_r} = 3.3 \quad (1)$$

Therefore the inlet velocity at reduced scale was multiplied by 3.3 and air flow rate was divided by 3.3.

The reduced-scale trailer (with a glass side wall) was loaded with 430 reduced-scale half-carcasses made of polyurethane (foam). They were obtained using a mold of a carcass produced by 3D printing based on an X-ray scan of a full-scale half-carcass (Figure 2).

The heat transfer in the studied configuration is mainly driven by convection between the blown air and the carcasses. Both natural and forced convection are involved in the heat transfer according to the velocity encountered in the full scale semitrailer which can be lower than $0.1 \text{ m}\cdot\text{s}^{-1}$. Indeed, for this value of velocity, the full scale Richardson number is higher than 1 ($\text{Ri}_f = 3.3$ for $\Delta T_f = 5^\circ\text{C}$, $L = 0.2 \text{ m}$, $v = 0.1 \text{ m}\cdot\text{s}^{-1}$) meaning that the natural and forced convections are the same order of magnitude. If natural convection should be taken into account in this study, the Grashof number in the reduced-scale trailer should also be the same as that in the full-scale trailer.

$$\text{Gr} = \frac{g \beta \Delta T L^3}{\nu^2} \quad (2)$$

where g is the gravitational acceleration, β the thermal expansion coefficient, ΔT the temperature difference between the carcass surface and the internal air, L a characteristic length and ν the kinematic viscosity. As the fluid used in both full and reduced scales is air, $\beta_f = \beta_r$ and $\nu_f = \nu_r$. The Grashof number conservation would imply that $\Delta T_r = (L_f/L_r)^3 \Delta T_f \approx 36 \Delta T_f$ where ΔT_r and ΔT_f are respectively temperature differences in the reduced-scale and the full-scale trailers, and L_f and L_r are respectively the characteristic lengths of the full-scale and the reduced-scale trailers. In the case of $\Delta T_f = 5^\circ\text{C}$, ΔT_r would be around 180°C . Because of technical feasibility, natural convection could not be reproduced in the reduced-scale trailer. Indeed, if the same ΔT in reduced and full scales is considered, the Richardson number in the reduced scale would be $3.3^3=36$ times lower than that of the full scale ($\text{Ri}_r < 0.1$). Thus, natural convection can be considered as negligible at reduced scale.

Two different air inlet configurations were used in this study: with and without air ducts. The configuration with two rectangular ducts ($0.2 \text{ m} \times 0.16 \text{ m} \times 6 \text{ m}$) is similar to some configurations encountered in France for carcass transportation. Both configurations have a symmetry plane so that the experimental investigations and the numerical simulations (to be presented in future work) can be conducted only on one half of the trailer. In the case without an air duct, the entire airflow is blown at $x = 0 \text{ m}$ (front of the trailer). In the case of the trailer with air ducts, 63% of the airflow is blown at $x = 0 \text{ m}$ (front) and 37% is blown at $x = 6 \text{ m}$ at the outlets of the two distribution ducts. Those dimensions correspond to the full-scale trailer.

2.1.2. Instrumented half-carcasses

The method developed for the measurement of heat convection coefficients on the carcasses, similar to those used in previous studies (Kondjoyan and Daudin, 1997, Willix et al., 2006), consists of heating continuously instrumented half-carcasses until a steady state is reached (constant temperature). The CHTC can be calculated using the measured heat flow and the recorded temperature difference between the surface of the carcass and the surrounding air according to Newton's law: $q/A = h (T_s - T_{air})$ (3)

Two reduced-scale plaster half-carcasses were manufactured as shown in Figure 3a. Two silicone heating panels (Vulcanic-France), each with a customized shape and a maximum heating capacity of 96 W were incorporated inside the plaster mass to ensure uniform heating to the greatest possible extent. Previously calibrated T-type thermocouples (200 μm of diameter) were placed just under the surface (less than 1 mm under the surface) of the plaster near the flow meters. The ambient air temperature was measured at 2 cm above and under the plaster half carcass (Figure 3). To calculate the CHTC for the ham part the air temperature above the half carcass was used. For the loin part the average air temperature was used.

Circular (30 mm diameter) copper-surface heat flux sensors (Captec-France) with T-type thermocouples were bonded to the surface of the plaster half-carcasses. The nominal sensitivity of each flow meter has been provided by the manufacturer, and this value is greater than $0.6 \mu\text{V} \cdot \text{W}^{-1} \cdot \text{m}^2$. The specific value obtained with each heat flux sensor makes it possible to convert the output signal from μV into $\text{W} \cdot \text{m}^{-2}$. Each plaster half-carcass was hung with a half-carcass made of polyurethane (Figure 3b).

The heat transfer coefficient in the full-scale trailer (h_f) was determined using Nusselt's analogy. Because Nu is a function of the Re and Pr numbers, and since $\text{Re}_f = \text{Re}_r$ and $\text{Pr}_f = \text{Pr}_r$:

$$\text{Nu}_r = \frac{h_r L_r}{\lambda_r} = \text{Nu}_f = \frac{h_f L_f}{\lambda_f} \rightarrow \frac{h_f}{h_r} = \frac{L_r \lambda_f}{L_f \lambda_r}$$

Air conductivity (λ_r) in the reduced-scale trailer where the mean temperature of the air is around 20°C is $0.0256 \text{ W} \cdot \text{m}^{-1} \cdot \text{K}^{-1}$. In a full-scale trailer during transport, the air temperature is around 4°C , which implies an air conductivity (λ_f) of $0.0243 \text{ W} \cdot \text{m}^{-2} \cdot \text{K}^{-1}$. Thus, we can obtain the following equation $\frac{h_f}{h_r} \approx \frac{1}{3.325}$ (4)

According to Daudin and Kuitche (1996), the energy exchanged by radiation is much lower than the energy exchanged by convection under the usual chilling conditions. In the case of a product surrounded by others at similar temperatures such as in our case, radiation is much lower (Kondjoyan, 2006) and can be neglected. However the part of the carcasses near the walls, the ceiling or the floor, whose temperature can be significantly different from the product surface area, are submitted to radiative heat transfer with them. In our case, the CHTC measurement positions are not located in these zones; the flux meters are always in front of other carcasses.

2.2. Experimental conditions

The measurements positions were located on half of the reduced scale trailer assuming the same phenomena in the other half because of the presence of a symmetry plane in the studied configurations. The two instrumented half-carcasses made of plaster were firstly placed in the reduced-scale trailer loaded with foam half-carcasses (428 half-carcasses + 2 plaster half-carcasses) in different positions (Figure 4). These two half-carcasses were heated using a heating capacity of 45 W for 45 minutes before starting the blowing of the trailer with a reference flow rate of $5500 \text{ m}^3 \cdot \text{h}^{-1}$ (full-scale value). Temperature and heat flux sensor output signal acquisitions were performed every minute using a data-logger (Keysight 34970A) and acquisition software (Agilent bench link data). It took 6 h to reach steady state. Then the data were recorded during a 1-h stationary phase.

Preliminary tests were carried out at the position $x^* = 3/8$ in order to check the repeatability and reproducibility of the measurement of the CHTC values to validate the experimental protocol. The repeatability was checked by repeating the operations explained in the previous paragraph on three successive days without removing the instrumented carcasses from the trailer. The reproducibility test involved the removal and repositioning of the instrumented carcass in between two measurements.

In order to investigate the effect of the airflow rate on the CHTC values, additional experiments have been carried out at three positions (i.e. $x^* = 6/8$, $7/8$ and x_{max}^*) in the trailer without air ducts. For those experiments, a reduced inlet airflow rate (half of the reference inlet airflow rate) has been used in order to represent the case of poor ventilation in the trailer. The CHTC values obtained were then compared with those obtained under the reference conditions of this study.

In all, 46 experiments were performed on the trailer without air ducts and 39 on the trailer with air ducts. All results shown in this paper were reported to the full-scale.

3. Results and discussion

3.1. Experimental repeatability and reproducibility

Three repeatability experiments were performed at $x^* = 3/8$ in the trailer without air ducts. The discrepancy of the results of these three experiments was not significant, whatever the position on the instrumented carcass (ham, loin and shoulder). The average standard deviation was about $0.14 \text{ W} \cdot \text{m}^{-2} \cdot \text{K}^{-1}$, whereas the largest difference was $0.55 \text{ W} \cdot \text{m}^{-2} \cdot \text{K}^{-1}$ (in the muscle part of the ham placed near the wall).

Three reproducibility experiments were performed at the same position ($x^* = 3/8$). There was good agreement between the obtained results on both instrumented half-carcasses; the average standard deviation was $0.3 \text{ W} \cdot \text{m}^{-2} \cdot \text{K}^{-1}$ and the difference was always less than $0.8 \text{ W} \cdot \text{m}^{-2} \cdot \text{K}^{-1}$.

The effect of the carcass's heating capacity on the CHTC was also investigated. Two heating capacities were tested (45 W and 90 W at $x^* = 1/8$) and the CHTC values obtained for different parts of the instrumented half-carcasses were compared. Results showed that the differences are 2% on the average and never exceed 5%. Thus, the discrepancy due to the heating capacity can be considered as non-significant as expected for forced convection and the capacity of 45 W was used in all the other experiments.

3.2. Overall view of the results

All measured local CHTC values throughout the trailer in both studied configurations (without or with air ducts) were summarized in Figure 5.

CHTC values varied according to the height in the carcass (ham, loin and shoulder), the side of the carcass (muscle or rind), the lateral position in the trailer (near the symmetry plane and near the lateral wall), the longitudinal position in the trailer (9 measuring positions from the front to the rear of the trailer) and the air blowing configuration (with or without air ducts).

The maximum values were obtained on the ham muscle side of the half-carcass placed near the symmetry plane in both studied configurations. In the trailer without air ducts $h_{\max} = 29.7 \text{ W} \cdot \text{m}^{-2} \cdot \text{K}^{-1}$ in the middle of the trailer and in the presence of air ducts, and $h_{\max} = 37.1 \text{ W} \cdot \text{m}^{-2} \cdot \text{K}^{-1}$ was obtained at the rear of trailer.

Minimum CHTC values were also obtained on the surface of the half-carcass placed near the symmetry plane in both studied configurations. Low CHTC values were obtained on the loin muscle side, at the rear of the trailer without air ducts ($h_{\min} = 1.68 \text{ W} \cdot \text{m}^{-2} \cdot \text{K}^{-1}$) and at $x^* = 6/8$ on the shoulder muscle side in the trailer with air ducts ($h_{\min} = 0.97 \text{ W} \cdot \text{m}^{-2} \cdot \text{K}^{-1}$).

It has to be kept in mind that these values of CHTC are given for full scale but there were extrapolated from CHTC measurement at reduced scale where free convection is always

It has to be kept in mind that these values of CHTC are given for full scale. These values were obtained by extrapolation from CHTC measurement at reduced scale where free convection is almost negligible. In fact, in real conditions (full scale trailer), free convection can contribute to increase significantly the CHTC. From literature correlation in similar conditions (vertical plate, $L = 0.2 \text{ m}$, $\Delta T = 5 \text{ }^\circ\text{C}$), CHTC values for free convection are indeed around $3 \text{ W} \cdot \text{m}^{-2} \cdot \text{K}^{-1}$.

Because of the complexity of airflow in our study, CHTC varies locally in a complex manner. In order to provide a better understanding, mean values have been calculated and are shown in Section 3.3.

3.3. Effect of the location on the surface of the carcasses

In order to appreciate the effect of the heat flux sensor position on the surface of the instrumented half-carcass on the measured CHTC, a mean value throughout the trailer (in both studied configurations) is represented in Figure 6.

In order to calculate mean values, the height position of the carcass was designed by the index i (1: muscle, 2: loin, 3: shoulder), the side position on the carcass was designed by the index j (1: muscle side, 2: rind side), the lateral position in the trailer was designed by the index k (1: near the symmetry plane, 2: near the wall), the longitudinal position in the trailer was designed by the index l (1: $x^*=x^*_{\min}=0.02$, 2: $x^*=1/8$, 3: $x^*=2/8$, 4: $x^*=3/8$, 5: $x^*=4/8$, 6: $x^*=5/8$, 7: $x^*=6/8$, 8: $x^*=7/8$, 9: $x^*=x^*_{\max}=0.96$) and the blowing configuration was designed by the index m , (1: without air ducts, 2: with air ducts). The average values of CHTC along the truck, as they are represented in Figure 6, correspond to the following expression:

$$\overline{h_{i,j,k,m}} = \sum_{l=1}^{l_{\max}} h_{i,j,k,l,m} / l_{\max} \quad (5)$$

Minimum, maximum and average from ham, loin and shoulder part CHTC values were calculated using expressions (6), (7) and (8).

$$\text{CHTC}_{\min} = \min_{l,k,m} \bar{h}_{i,k,l,m}^j \quad \text{where} \quad \bar{h}_{i,k,l,m}^j = \sum_{j=1}^2 h_{i,j,k,l,m} / 2 \quad (6)$$

$$\text{CHTC}_{\max} = \max_{l,k,m} \bar{h}_{i,k,l,m}^j \quad (7)$$

$$\text{CHTC}_{\text{ave}} = \bar{h}^{j,k,l,m} = \sum_{j=1}^2 \sum_{k=1}^2 \sum_{l=1}^{l_{\max}} \sum_{m=1}^2 h_{i,j,k,l,m} / (2^3 l_{\max}) \quad (8)$$

Figure 6 shows a large variation in the mean values between the ham, loin and shoulder parts in both studied configurations. Results were significantly higher in the ham part (min. $3.4 \text{ W.m}^{-2}.\text{K}^{-1}$, max $22.6 \text{ W.m}^{-2}.\text{K}^{-1}$, average $12.6 \text{ W.m}^{-2}.\text{K}^{-1}$) than in the loin part (min. $1.9 \text{ W.m}^{-2}.\text{K}^{-1}$, max $7.7 \text{ W.m}^{-2}.\text{K}^{-1}$, average $6.0 \text{ W.m}^{-2}.\text{K}^{-1}$) and in the shoulder part (min. $4.2 \text{ W.m}^{-2}.\text{K}^{-1}$, max $7.4 \text{ W.m}^{-2}.\text{K}^{-1}$, average $5.8 \text{ W.m}^{-2}.\text{K}^{-1}$).

This is due to the fact that air is blown above the carcasses near the ceiling of the trailer and flows with relatively high velocities (most often $> 2 \text{ m.s}^{-1}$, Merai et al. 2018).

Considering the ham, the observed CHTC values were higher on the muscle side (min. $15.8 \text{ W.m}^{-2}.\text{K}^{-1}$, max $22.6 \text{ W.m}^{-2}.\text{K}^{-1}$, average $18.0 \text{ W.m}^{-2}.\text{K}^{-1}$) than on the rind side (min. $3.4 \text{ W.m}^{-2}.\text{K}^{-1}$, max $11.3 \text{ W.m}^{-2}.\text{K}^{-1}$, average $7.2 \text{ W.m}^{-2}.\text{K}^{-1}$) in both configurations. This is mainly due to the fact that with the suspension system used, the rind side of the ham part of a carcass is in contact with the rind side of another carcass, whereas there is a greater air space between the muscle sides of the two half-carcasses, thus allowing a higher airflow rate.

CHTC variations between the muscle and rind sides of the loin and the shoulder parts were lower ($\leq 4.5 \text{ W.m}^{-2}.\text{K}^{-1}$, Figure 6).

CHTC variations are mainly related to the characteristics of the airflow around the carcasses (particularly air velocity) and to the characteristics of the product itself (shape, dimensions, position relative to airflow direction) (Verboven et al., 1997). These observations are similar to those of Kondjoyan, 2006: for the same carcass, some parts are exposed to high air velocity while others are exposed to almost stagnant air.

The overall average CHTC values in the cases with ducts and without ducts are similar ($7.7 \text{ W} \cdot \text{m}^{-2} \cdot \text{K}^{-1}$ and $8.5 \text{ W} \cdot \text{m}^{-2} \cdot \text{K}^{-1}$, respectively).

3.4. Relationship between convective heat transfer coefficient and airflow pattern

In order to understand the effect of local air velocity (measured by LDV, already presented in Merai et al, 2018) on the CHTC value, the following analysis was carried out.

3.4.1. Trailer without air ducts

As presented in Section 3.2, the CHTC value varies according to the position on the same carcass. Figure 7a shows the variation in this measured coefficient for the ham, loin and shoulder along the trailer. The presented values are the mean of both the muscle and the rind sides of the carcass located on the symmetry plane and near the side wall. These values were analyzed by comparing them with the simplified airflow pattern (Figure 7b) in which the dimensionless airflow is shown (Merai et al., 2018). This dimensionless airflow was defined as the ratio between the airflow rate at a given position and the airflow rate at the inlet.

High dimensionless airflow values were obtained on the top of the carcasses (ham parts) compared with the loin and shoulder parts. On the top of the carcasses, the dimensionless airflow increased from the blowing at the inlet of the trailer ($x^* = 0$) to $x^* = 4/8$. At this position, the airflow separates into 2 streams with different airflow rates: ceiling (low airflow rate) and downward vertical airflow (high airflow rate) throughout the carcasses. This explains the increase in CHTC values on the surface of the ham parts, and the maximum value at $x^* = 4/8$.

Stable mean CHTC values were obtained for both loin and shoulder ($\approx 7 \text{ W} \cdot \text{m}^{-2} \cdot \text{K}^{-1}$) because of the low airflow rate (vertical and horizontal flow) in the bottom part of the trailer. At the front of the trailer ($x^* \approx 0$), the higher CHTC value for the shoulder compared with that for the loin can be explained by entrainment of the air from the bottom to the top of the carcasses due to the strong blowing.

It is important to note that the lowest CHTC values are not necessarily in the rear part of the trailer as observed by Moureh and Flick (2005) in the case of a trailer loaded with pallets. In fact, about 32% of the airflow was directed to the rear of the trailer and goes down in the empty space between the last carcasses and the trailer door. This explains the relative high CHTC for the ham at the rear of the trailer; see Figure 7a the increase of CHTC for ham $x^* = 5/8$ to x^*_{max} .

In order to illustrate CHTC differences according to the lateral position, Figure 8 compares the evolution of CHTC on the muscle side of the ham part near the symmetry plane and near the lateral wall. Overall, the CHTC (on the muscle side of the ham) is higher near the symmetry plane (average $23 \text{ W} \cdot \text{m}^{-2} \cdot \text{K}^{-1}$) than near the wall (average $16 \text{ W} \cdot \text{m}^{-2} \cdot \text{K}^{-1}$). However, the opposite is true at the particular location $x^* = 1/8$.

These results can be explained by the velocity profile obtained using LDV on the top of the carcasses at positions $x^* = 1/8$ (Figure 8b) and $x^* = 5/8$ (Figure 8c). For $x^* = 1/8$; the vertical

velocity on the top of carcasses is higher near the side wall than near the symmetry plane; whereas for $x^* = 5/8$, the vertical velocity is higher near the symmetry plane than near the side wall.

This illustrates that some of the trends observed for the CHTC can be explained by the previous velocity measurements using LDV (Merai et al., 2018). However, other CHTC variations could not be explained by the simplified flow pattern scheme (Figure 7a) or by measurements conducted above the carcasses (Figure 8a).

It would be interesting to correlate the local CHTC values obtained with the local velocity near to the carcasses. However, it was not possible to measure air velocity close to the carcass surfaces using LDV. A future computational fluid dynamic study (CFD model) will be conducted to estimate the relationship between local CHTC values and local velocities.

3.4.2. Trailer with air ducts

The same approach was used for the trailer with air ducts in order to analyze the effect of airflow characteristics on the CHTC. The CHTC values for different parts of the carcass (ham, loin and shoulder) are shown in Figure 9a (mean values on both rind and muscle sides for the carcasses located near the symmetry plane and near the side wall).

Similarly to the case without an air duct, the ham part presents the highest CHTC. The values increased at the front of the trailer ($0 < x^* \leq 2/8$) because of the entrainment effect of the air jet blown from the first air inlet. The value decreased for $2/8 < x^* \leq 5/8$ and then increased again for $x^* > 5/8$ because of the air blown from the distribution duct located at this position. The same trend was observed for the shoulder and loin parts along the trailer. However, CHTC values were much lower for the loin and shoulder parts compared with the ham parts. The lowest values ($\approx 3.2 \text{ W} \cdot \text{m}^{-2} \cdot \text{K}^{-1}$) were obtained at $x^* = 5/8$ where a stagnant airflow was observed in the simplified airflow of the trailer with air ducts (Figure 9b).

By comparing the results shown in Figure 7a (without an air duct) and Figure 9a (with an air duct), it can be seen that the presence of air ducts does not improve the homogeneity of the CHTC values obtained. However, these results depend on the empty space between the last carcass and the rear door of the trailer (0.45 m in our study) which allows a significant part of the blown air to reach the rear part of the trailer. If this empty space at the rear is reduced, it is expected that the rear part of the trailer will be less ventilated.

3.5. Effect of the airflow rate

Additional measurements were conducted at $x^* = 6/8$, $7/8$ and x_{max}^* with only 50% of the reference airflow rate. The aim was to investigate the impact of lower air velocity on the CHTC. In practice, the airflow rate may vary due to the trailer design, and some trailers offer a choice of two airflow rates.

The ratio of the CHTC values obtained with the full airflow rate (h) and the half airflow rate ($h_{1/2}$), had an average of 1.57 with a standard deviation of 0.48.

For pork hindquarters, Kondjoyan and Daudin (1997) found that CHTC is proportional to the velocity at power 0.73, so doubling the flow rate should multiply the CHTC by 1.7 which is slightly different from the average ratio obtained here. Kondjoyan and Daudin (1997) conducted their study on a single hindquarter with controlled air velocity, turbulence and angle of exposure. In this study, because of the complex airflow pattern in terms of velocity and turbulence when the airflow rate is halved, the velocity around a given carcass is not necessarily half of the reference velocity in all places. In fact, the airflow pattern could change completely and exert an important effect on the local velocities.

4. Conclusion and perspectives

A methodology for convective heat transfer coefficient measurement was developed using a steady state method. The method was applied to the case of pork carcasses loaded in a trailer. Instrumented plaster carcasses were made, and heat flux sensors were placed on different parts of the carcass (ham, loin and shoulder) on the muscle and rind sides. These carcasses were placed at different positions in a reduced-scale trailer (1:3.3) loaded with carcasses made of polyurethane representing airflow obstacles. Two configurations were studied: with and without air distribution ducts.

For the ham part, almost everywhere in the trailer, the convective heat transfer coefficient on the rind side was lower than that on the muscle side. This is mainly due to the fact that with the suspension system used, two carcasses located side-by-side are in contact on the rind side of the ham part; this led to low airflow on this side. A greater air space between the muscle sides allows better air circulation between the half-carcasses. The effect of air ducts on the convective heat transfer coefficient is not significant for both loin and shoulder parts. Values were almost stable along the trailer with mean values of 5-7 W.m⁻².K⁻¹.

In future studies, 3D modelling will be developed by combining the conduction inside the carcasses and the convection with the surrounding environment. The experimentally determined CHTC value obtained in the present study will be useful in order to introduce realistic boundary conditions. This model will be associated with a predictive microbial model to evaluate the health risk for consumers in different transport scenarios (initial temperature, air temperature and humidity, transport duration).

Acknowledgement

This research work was carried out within the framework of a DIM ASTREA grant by the Regional Council of Ile-de-France (France).

References

Anonymous, 2004. Regulation (EC) No 853/2004 of the European Parliament and of the Council of 29 April 2004 laying down specific hygiene rules for food of animal origin. Official Journal of the European Union 001.001/001–059.

- Carniol, N., Kondjoyan, A., Daudin, J.D., Alvarez, G. and Bimbenet, J.J., 2000. Heat transfer coefficient distribution inside finite height cylinders array under a highly turbulent air free stream. *Entropie*. 227, 42-52.
- Daudin, J.D., and Kuitche, A., 1996. Modelling of temperature and weight loss kinetics during meat chilling for time variable conditions using analytical based method-II. Calculations versus measurements on pork carcass hindquarters. *Journal of Food Engineering*. 29 (1), 39-62.
- Duret, S., Hoang, H-M., Flick, D., and Laguerre, O., 2014. Experimental characterization of airflow, heat and mass transfer in a cold room filled with food products. *International Journal of Refrigeration*. 46, 17-25.
- EFSA BIOHAZ Panel, 2014. Scientific opinion on the public health risks related to the maintenance of the cold chain during storage and transport of meat. Part 1 (meat of domestic ungulates). *EFSA Journal* 2014, 12 (3):3601, 81. doi:10.2903/j.efsa.2014.3601.
- Ghisalberti, L., and Kondjoyan, A., 1999. Convective heat transfer coefficients between air flow and a short cylinder. Effect of air velocity and turbulence. Effect of body shape, dimensions and position in the flow. *Journal of Food Engineering*. 42, 33-44.
- Harris, M.B., Carson, J.K., Willix, J., and Lovatt S.J., 2004. Local surface heat transfer coefficients on a model lamb carcass. *Journal of Food Engineering*. 61, 421-429.
- James, S. 1996. The chill chain “from carcass to consumer”. *Meat Science*. 43, 203-216.
- Kondjoyan, A., and Daudin, J.D., 1997. Heat and mass transfer coefficients at the surface of a pork hindquarter. *Journal of Food Engineering*. 32, 225-240.
- Kondjoyan, A., 2006. A review on surface heat and mass transfer coefficients during air chilling and storage of food products. *International Journal of Refrigeration*. 29, 863-875.
- Merai, M., Flick, D., Guillier, L., Duret, S., and Laguerre, O., 2018. Experimental characterization of airflow inside a refrigerated trailer loaded with carcasses. *International Journal of Refrigeration*, 88, 337-346.
- Moureh, J., Flick, D., 2005. Airflow characteristics within a slot-ventilated enclosure. *International Journal of Heat and Fluid Flow*. 26, 12-24.
- Savell, J.W., Mueller, S.L., Baird, B.E., 2005. The chilling of carcasses. *Meat Science* 70 (3), 449-459.
- Verboven, P., Nicolai, B., Scheerlinck, N., and De Baerdemaeker, J., 1997. The local surface heat transfer coefficient in thermal food process calculations: a CFD approach. *Journal of Food Engineering*. 33, 15-35.
- Willix, J., Harris, M.B., and Carson, J.K., 2006. Local surface heat transfer coefficients on a model beef side. *Journal of Food Engineering*. 74, 561-567.

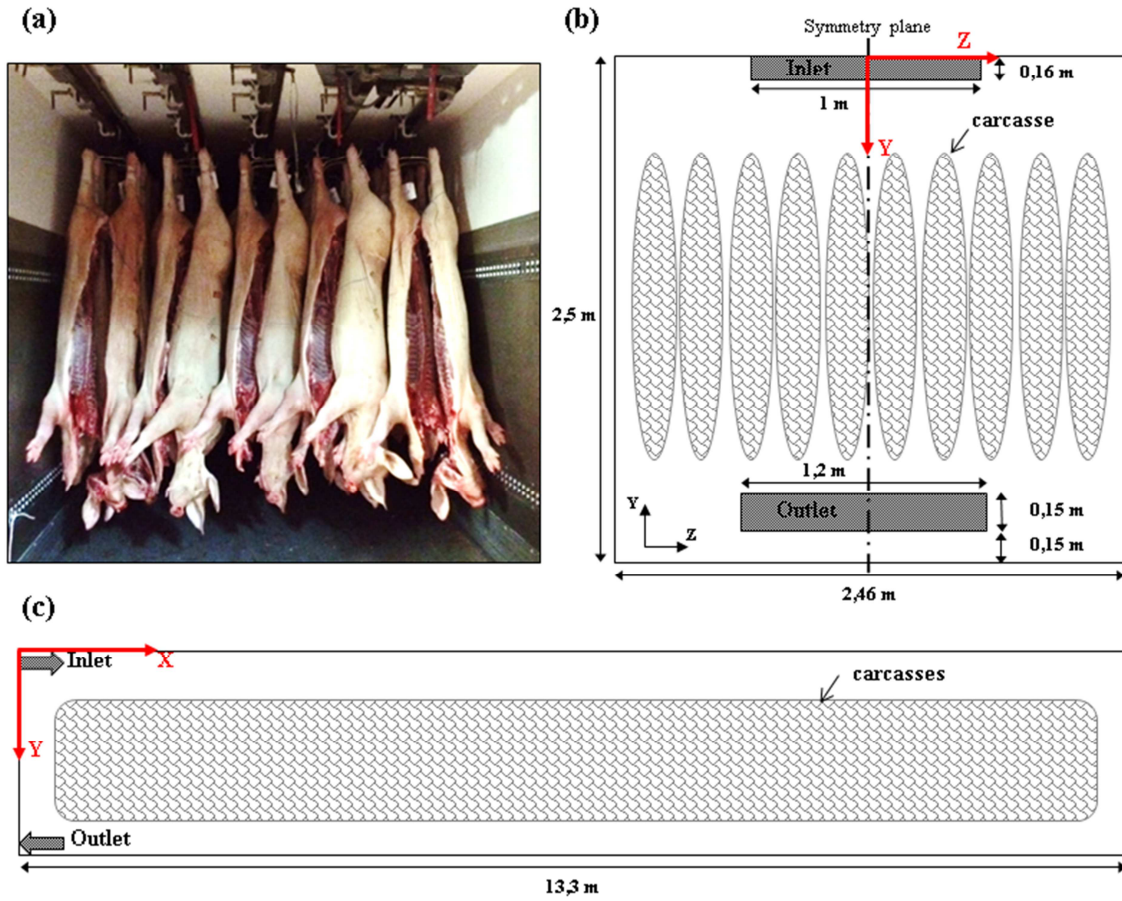


Figure 1. Loaded trailer; (a) real scale of the chosen configuration; (b) front view and (c) side view with characteristic dimensions.

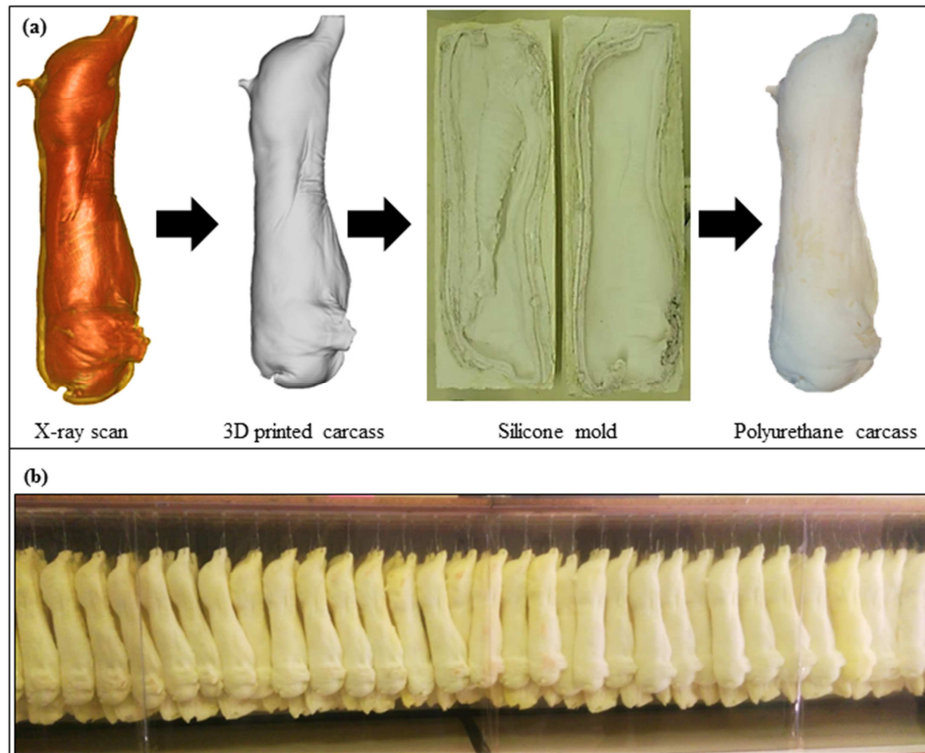


Figure 2. (a): Steps in the production of reduced-scale carcasses based on the X-ray scan of a real pork carcass (b): Side view of the reduced-scale trailer loaded with reduced-scale carcasses.

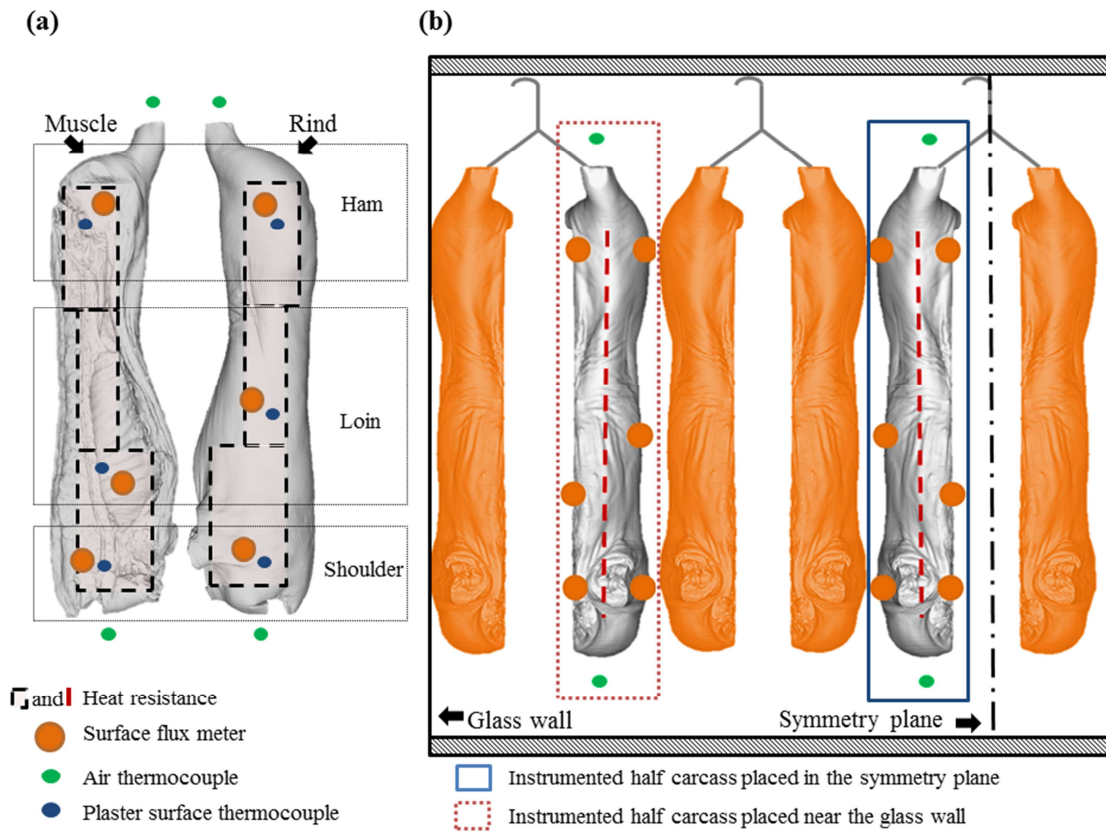


Figure 3. Instrumentation of the plaster half-carcasses (a) location of the heating panels, heat flux sensors, surface thermocouples and ambient air; (b) positions of the plaster half-carcass and the polyurethane ones.

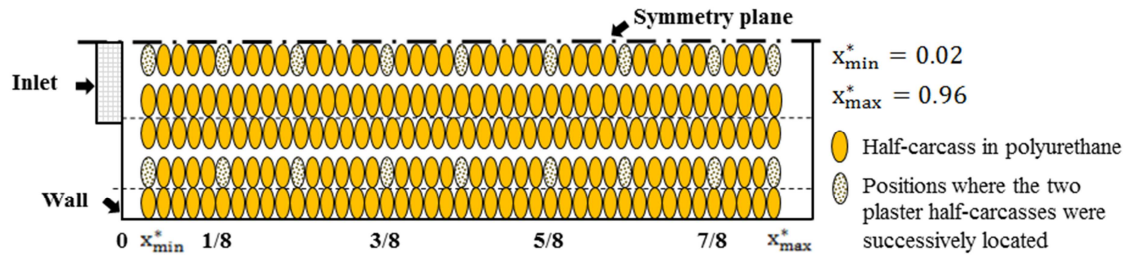


Figure 4. Top view of half of the trailer loaded with half-carcasses showing the measurement positions used to measure the CHTC using instrumented plaster half-carcasses.

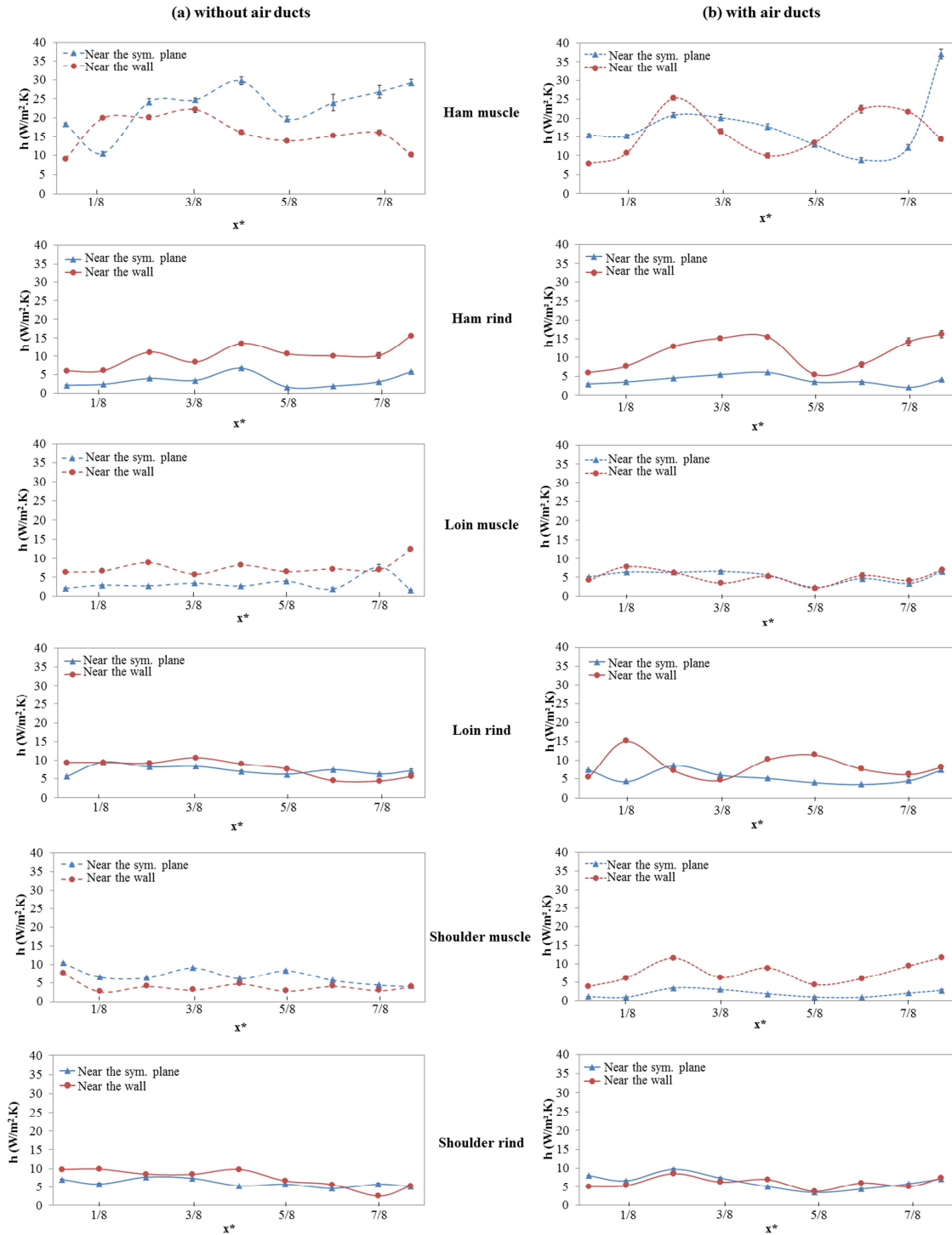


Figure 5. Local CHTC measured on the muscle and rind surfaces of the ham, loin and shoulder parts of the instrumented half-carcaasses in the trailer (a) without air ducts and (b) with air ducts.

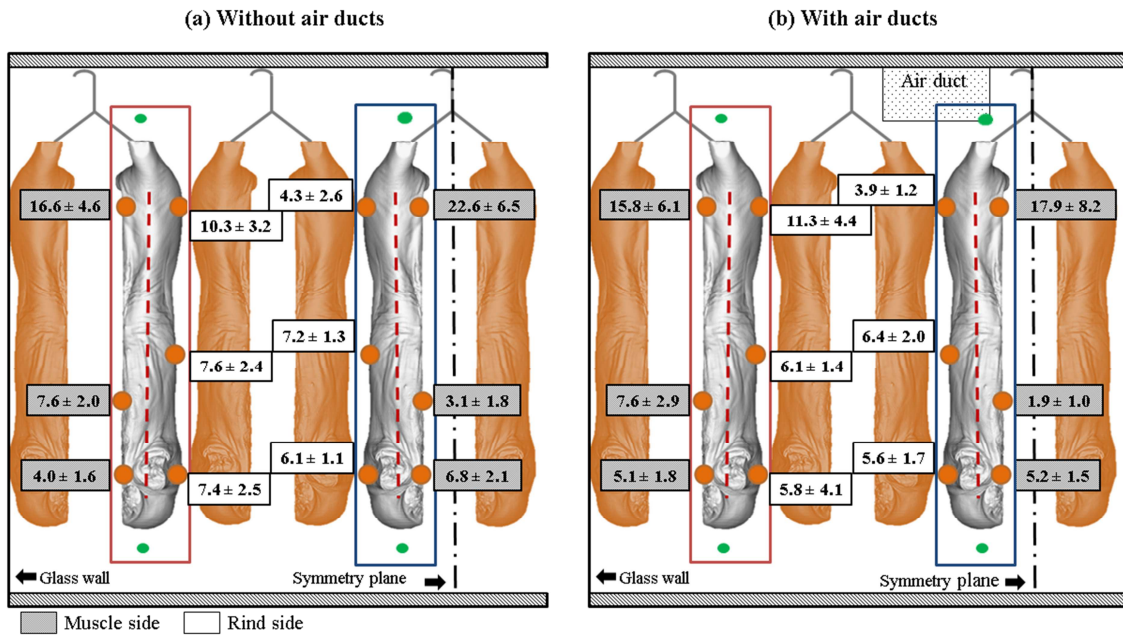


Figure 6. Mean CHTC values ($W \cdot m^{-2} \cdot K^{-1}$) along the trailer and their standard deviation at different positions of the instrumented half-carass. (a) without air ducts, and (b) with air ducts.

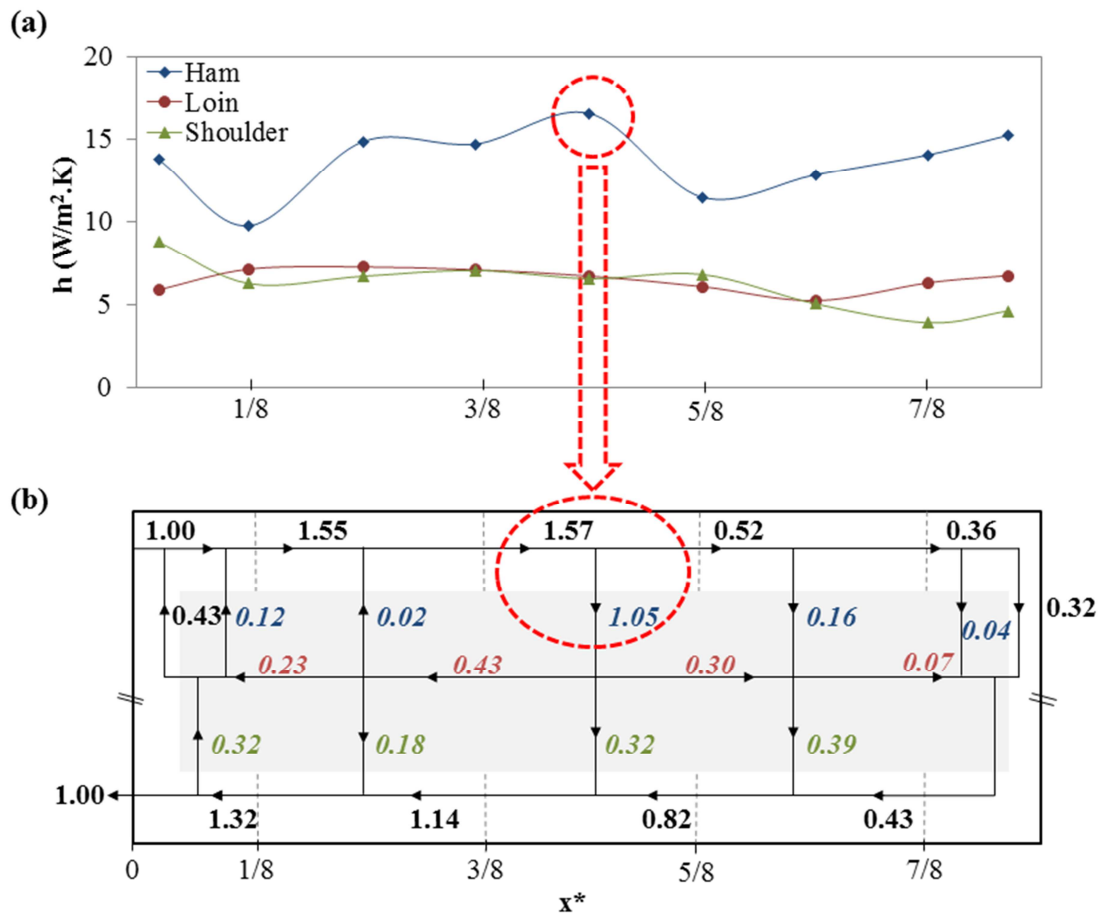


Figure 7. (a) CHTC (mean values for rind and muscle sides of carcasses located near the symmetry plane and near the wall) along the trailer without air ducts at the surface of ham (blue \diamond), loin (red \blacksquare) and shoulder (green \blacktriangle), (b) Simplified airflow pattern in the trailer loaded with carcasses without air ducts (values represent dimensionless airflow rates).

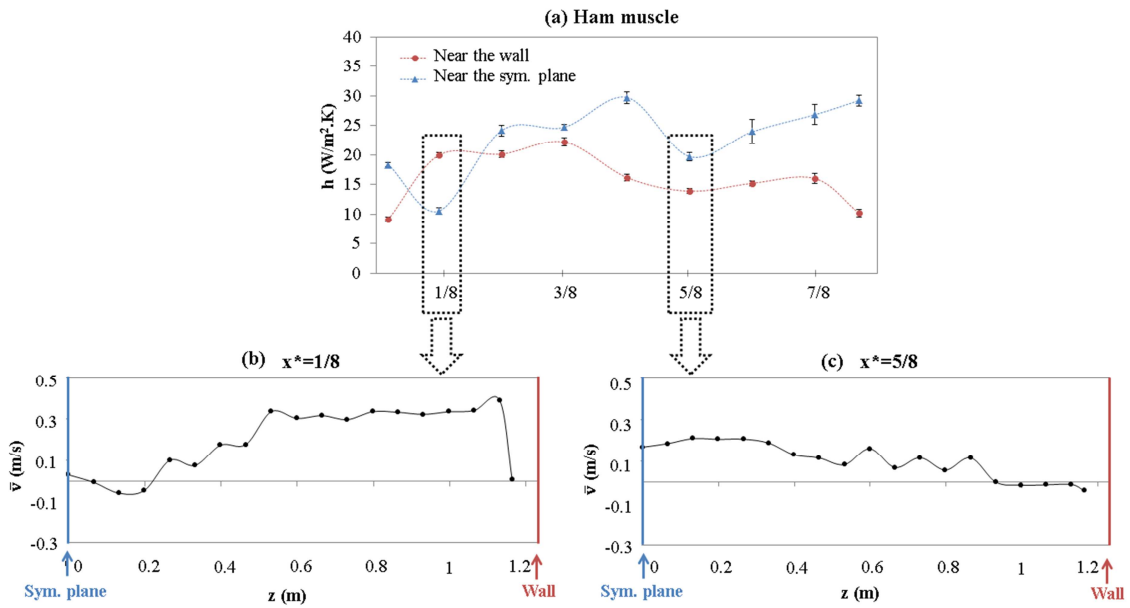


Figure 8. (a) CHTC at muscle side of ham of the carcasses near the side wall (red ●) and near the symmetry plane (blue ■), (b) Vertical time averaged velocity (positive downwards) on the top of carcasses at $x^* = 1/8$ and (c) at $x^* = 5/8$.

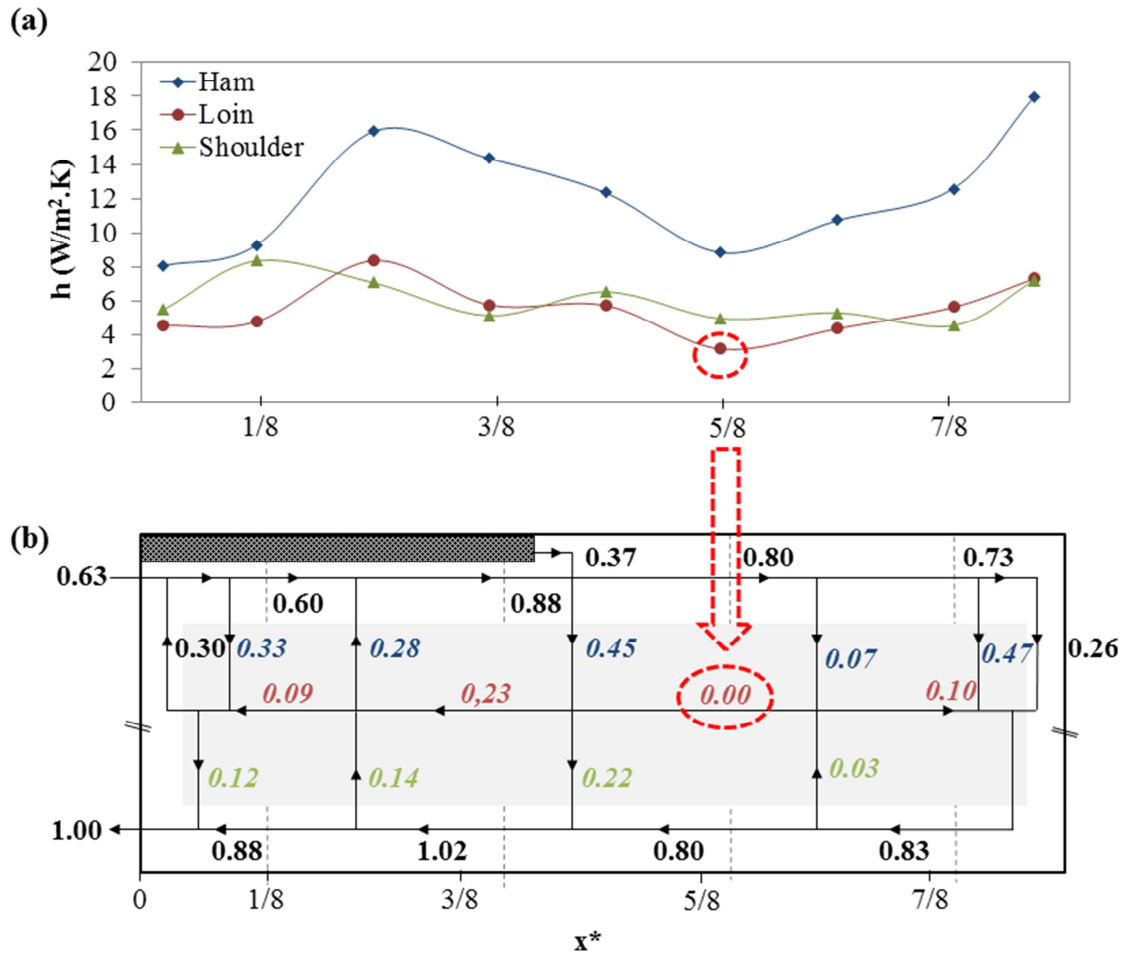


Figure 9. (a) CHTC (mean values for rind and muscle sides of carcasses located near the symmetry plan and near the side wall) along the trailer with air ducts at the surface of ham (bleu \blacklozenge), loin (red \blacksquare) and shoulder (green \blacktriangle), (b) Simplified airflow direction in the trailer loaded with carcasses with air ducts (values represent dimensionless airflow rates).